Science Advances

advances.sciencemag.org/cgi/content/full/4/9/eaau4640/DC1

Supplementary Materials for

A comprehensive portrait of the venom of the giant red bull ant, *Myrmecia gulosa*, reveals a hyperdiverse hymenopteran toxin gene family

Samuel D. Robinson*, Alexander Mueller, Daniel Clayton, Hana Starobova,
Brett R. Hamilton, Richard J. Payne, Irina Vetter,
Glenn F. King, Eivind A. B. Undheim*

*Corresponding author. Email: sam.robinson@uq.edu.au (S.D.R.); e.undheim@uq.edu.au (E.A.B.U.)

The PDF file includes:

Supplementary Materials and Methods
Results
Fig. S1. MALDI-MS analysis of *M. gulosa* venom apparatus.
Fig. S2. Coelution of native (purified from venom) and synthetic $MIITX_1$-Mg1a.
Fig. S3. $MIITX_1$-Mg1a–induced changes in paw withdrawal.
Table S1. Venom- or toxin-associated annotation of nonvenom component transcripts.
Table S2. Assessment of antimicrobial, cytotoxic and hemolytic activity of $MIITX_1$-Mg1a.

Other Supplementary Material for this manuscript includes the following:

(available at advances.sciencemag.org/cgi/content/full/4/9/eaau4640/DC1)

Movie S1 (.mov format). Collection of venom from *M. gulosa*.

Supplementary Materials and Methods
Antimicrobial and cytotoxicity assays
Antimicrobial and cytotoxicity assays were performed by CO-ADD (The Community for Antimicrobial Drug Discovery). Briefly, growth inhibition of all bacterial strains was determined by measuring absorbance at 600 nm, growth inhibition of *C. albicans* was determined by measuring absorbance at 530 nm, and growth inhibition of *C. neoformans* was determined by measuring the difference in absorbance between 600 and 570 nm, after the addition of resazurin (0.001% final concentration) and incubation at 35°C for an additional 2 h. Growth inhibition of HEK293 cells was determined by measuring fluorescence (excitation 530/10 nm, emission 590/10 nm) after the addition of resazurin (25 µg/mL final concentration) and incubation at 37°C and 5% CO_2, for an additional 3 h. Percentage growth inhibition was calculated using negative controls (media only) and positive controls (no peptide). For the haemolytic activity assay, human whole blood was washed three times with 3 volumes of 0.9% NaCl and then resuspended in 0.9% NaCl to a concentration of 0.5 x 10^8 cells/mL. Cells were incubated for 1 h at 37°C with or without the peptide. After incubation, plates were centrifuged at 1000 *g* for 10 min to pellet cells and debris and haemolysis determined by measuring the supernatant absorbance at 405 nm. Minimum inhibitory concentration (MIC), CC_{50} (concentration at 50% cytotoxicity) and HC_{50} (concentration at 50% haemolytic activity) values were calculated by curve fitting the inhibition values versus log(concentration) using a sigmoidal dose-response function (variable slope), in Pipeline Pilot's dose-response component.

Results
**Antimicrobial activity of MIITX$_1$-Mg1a**
Several previously described ant venom peptides have been shown to have antimicrobial activity (*20*), and therefore we examined the potential utility of MIITX$_1$-Mg1a as an antimicrobial. MIITX$_1$-Mg1a was tested on a range of available microbial strains (**Table S2**). The peptide caused complete growth inhibition of the fungus *Cryptococcus neoformans var. grubii*, with an MIC of 2.5 µM. At the highest concentration tested (10.2 µM), it also partially inhibited growth of the bacteria *Staphylococcus aureus* and *Acinetobacter baumannii*, with 84 and 32% inhibition, respectively, but had no effect on the bacteria *Escherichia coli*, *Klebsiella pneumoniae*, *Pseudomonas aeruginosa*, or the fungus *Candida albicans*. At the highest concentration tested (10.2 µM), MIITX$_1$-Mg1a was not haemolytic (to human red blood cells), but it did display partial toxicity (49.1% growth inhibition) of HEK293 cells.
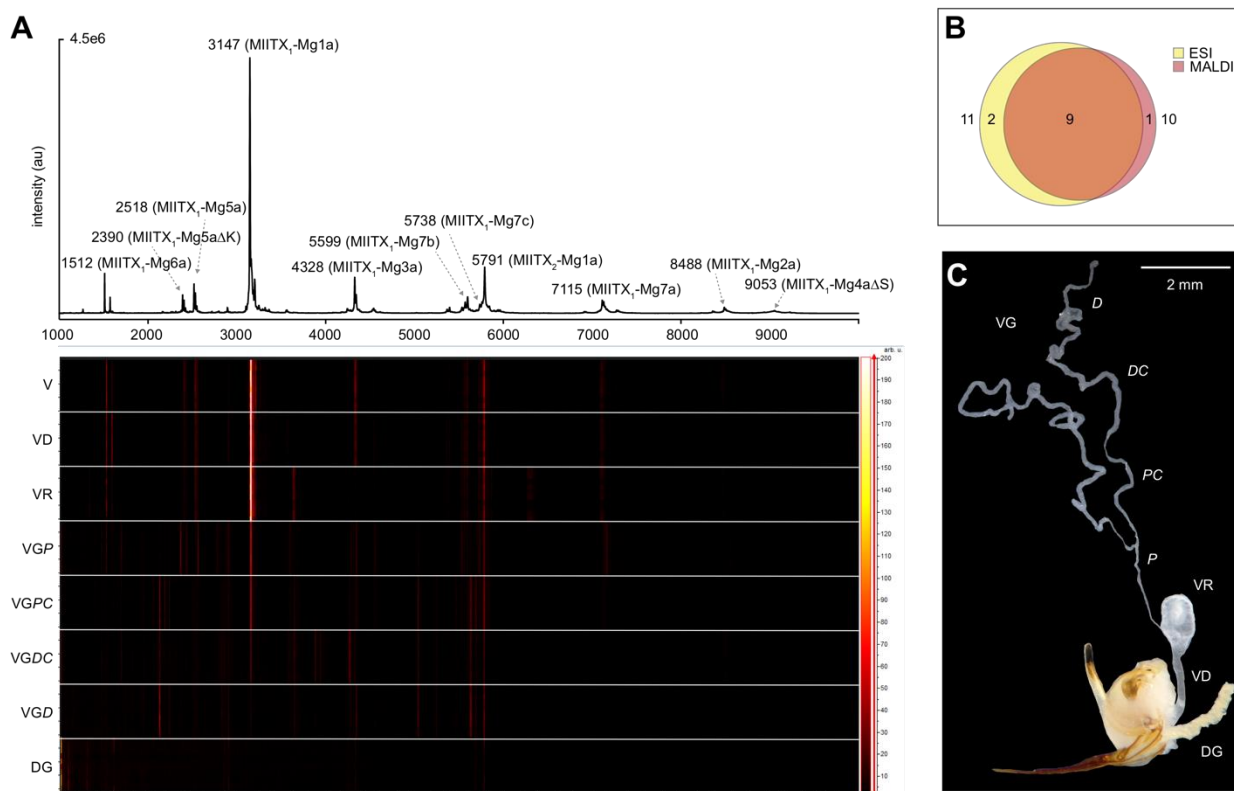
Fig. S1. MALDI-MS analysis of *M. gulosa* venom apparatus. (**A**) MALDI spectrum, generated in linear positive mode, of *M. gulosa* venom. Peaks corresponding to peptides identified as venom components by combined ESI-MS/transcriptomics are labelled. Theoretical MH_{av}^{+1} for each peptide are as follows: $MIITX_1$-Mg6a, 1511.9; $MIITX_1$-Mg5aΔK, 2390.9; $MIITX_1$-Mg5a, 2519.1; $MIITX_1$-Mg1a, 3147.8; $MIITX_1$-Mg3a, 4329.0; $MIITX_1$-Mg7b, 5600.4; $MIITX_1$-Mg7c, 5740.6; $MIITX_2$-Mg1a, 5792.3; $MIITX_1$-Mg7a, 7116.3; $MIITX_1$-Mg2a, 8489.4; $MIITX_1$-Mg4aΔS, 9054.1. Gel view (prepared in ClinProTools) illustrates variation across 10 individual shots of samples prepared from venom (V), venom duct (VD), venom reservoir (VR), Dufour's gland (DG) and 4 sections of the venom glands: proximal (VG*P*), proximal central (VG*PC*), distal central (VG*DC*) and distal (VG*D*). (**B**) Venn diagram illustrating overlap in peptides identified using different MS techniques. (**C**) Venom apparatus of *M. gulosa*, labelled as above.
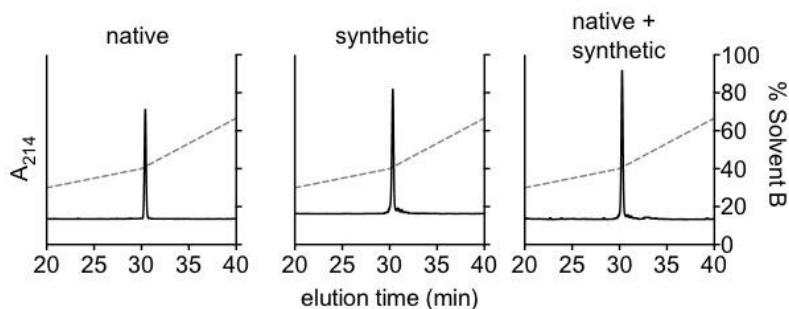
Fig. S2. Coelution of native (purified from venom) and synthetic $MIITX_1$-Mg1a. RP-HPLC was performed using a Phenomenex Gemini NX-C_{18} column (250 x 4.6 mm, 3 μm particle size, 110 Å pore size) with a gradient of 15–45% solvent B (90% ACN, 0.05% TFA) over 30 min.
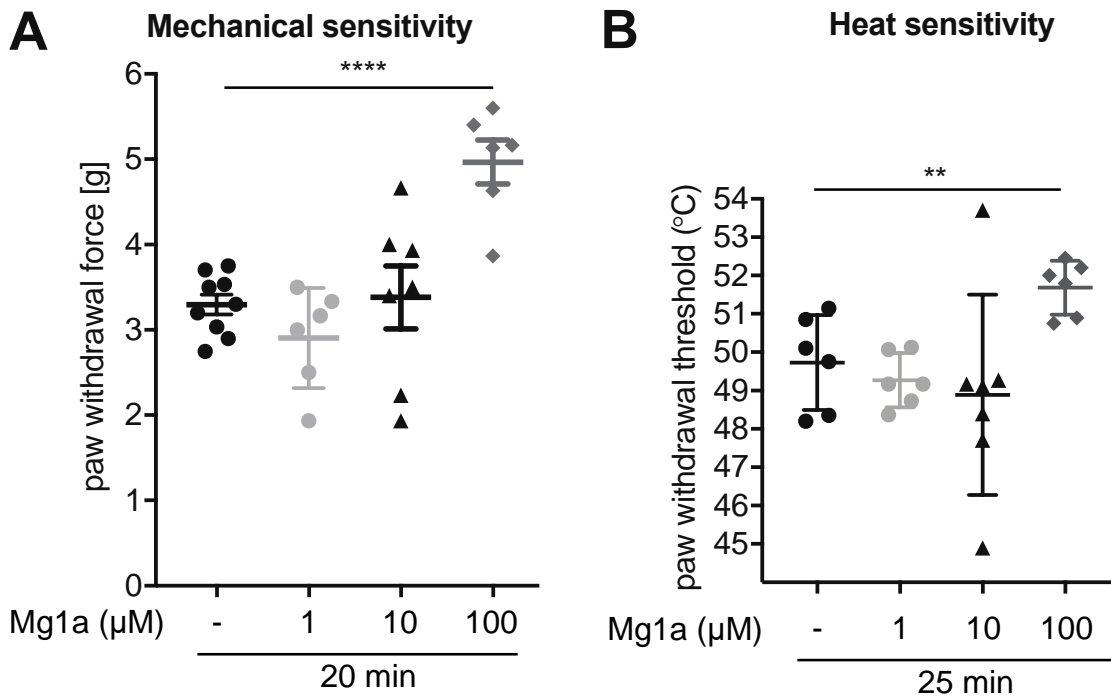
Fig. S3. MIITX$_1$-Mg1a–induced changes in paw withdrawal. (**A**) At a concentration of 100 μM, MIITX$_1$-Mg1a had caused mechanical sensitivity (at 20 min post-injection), $n = 3$–9 per group. (**B**) MIITX$_1$-Mg1a (100 μM) caused heat sensitivity (at 25 min post-injection). $n = 6$–7 per group. Data are expressed as mean ± SEM. Statistical significance compared to vehicle controls was determined using one-way ANOVA with Dunnett's multiple comparison test. ** $p < 0.01$, **** $p < 0.0001$.

Table S1. Venom- or toxin-associated annotation of nonvenom component transcripts.

UniProt Entry	Protein name	Organism	TPM
A7X3V4	Kunitz-type serine protease inhibitor kunitoxin-Tel1	*Telescopus dhara*	269.55
B2D0J5	Venom carboxylesterase-6	*Apis mellifera*	203.1
C9WMM5	Venom serine carboxypeptidase	*Apis mellifera*	152.1
Q58L94	Venom prothrombin activator notecarin-D2	*Notechis scutatus scutatus*	85.64
Q58L94	Venom prothrombin activator notecarin-D2	*Notechis scutatus scutatus*	70.75
B2D0J5	Venom carboxylesterase-6	*Apis mellifera*	54.33
B5U2W0	Venom serine protease Bi-V	*Bombus ignitus*	35.14
Q8T0W5	PIMHY Cysteine-rich venom protein 1	*Pimpla hypochondriaca*	29.79
P35779	Venom allergen 3	*Solenopsis richteri*	27.35
A7X3V4	Kunitz-type serine protease inhibitor kunitoxin-Tel1	*Telescopus dhara*	19.98
Q8MQS8	Venom serine protease 34	*Apis mellifera*	19.82
B5AJT4	Venom metalloproteinase 3	*Eulophus pennicornis*	18.3
C9WMM5	Venom serine carboxypeptidase	*Apis mellifera*	15.79
B5AJT4	Venom metalloproteinase 3	*Eulophus pennicornis*	13.95
Q8MQS8	Venom serine protease 34	*Apis mellifera*	13.06
Q8JI39	Cysteine-rich venom protein triflin	*Protobothrops flavoviridis*	10.95
B5AJT4	Venom metalloproteinase 3	*Eulophus pennicornis*	6.8
B5AJT4	Venom metalloproteinase 3	*Eulophus pennicornis*	6.71
B5AJT4	Venom metalloproteinase 3	*Eulophus pennicornis*	6.63
P0DM55	Venom peptide SjAPI	*Scorpiops jendeki*	5.64
Q8MQS8	Venom serine protease 34	*Apis mellifera*	5.05
B5AJT4	Venom metalloproteinase 3	*Eulophus pennicornis*	4.94
P505486	Conopressin	*Conus geographus*	3.95
B5AJT4	Venom metalloproteinase 3	*Eulophus pennicornis*	3.35
P35775	Venom allergen 2	*Solenopsis invicta*	1.61

Table S2. Assessment of antimicrobial, cytotoxic and hemolytic activity of MIITX$_1$-Mg1a.

Bacterium	Strain	Organism	Max response ± SEM	MIC (µM)
Staphylococcus aureus	ATCC 43300	Bacterium	84 ± 0	10.2
Escherichia coli	ATCC 25922	Bacterium	−1 ± 2	>10.2
Klebsiella pneumoniae	ATCC 700603	Bacterium	16 ± 1	>10.2
Acinetobacter baumannii	ATCC 19606	Bacterium	32 ± 3	>10.2
Pseudomonas aeruginosa	ATCC 27853	Bacterium	4 ± 4	>10.2
Candida albicans	ATCC 90028	Fungus	8 ± 4	>10.2
Cryptococcus neoformans var. grubii	H99; ATCC 208821	Fungus	108 ± 6	2.5
Human embryonic kidney cells	ATCC CRL-1573	Human	49 ± 7	8.8 (CC$_{50}$)
Human red blood cells		Human	10 ± 1	>10.2 (HC$_{50}$)

MIC, minimum inhibitory concentration; CC$_{50}$, concentration at 50% cytotoxic activity; HC$_{50}$, concentration at 50% haemolytic activity.